Stopping effects in U+U collisions with a beam energy of 520 MeV/nucleon

Xiao-Feng Luo,[1,*] Xin Dong,[1] Ming Shao,[1] Ke-Jun Wu,[2] Cheng Li,[1] Hong-Fang Chen,[1] and Hu-Shan Xu[3]

[1]*University of Science and Technology of China, Hefei, Anhui 230026, People's Republic of China*

[2]*Institute of Particle Physics, Hua-Zhong Normal University, Wuhan, Hubei 430079, People's Republic of China*

[3]*Institute of Modern Physics, Chinese Academy of Sciences, LanZhou, Gansu 730000, People's Republic of China*

(Received 1 April 2007; published 4 October 2007)

A relativistic transport model (ART1.0) is applied to simulate the stopping effects in tip-tip and body-body U+U collisions, at a beam kinetic energy of 520 MeV/nucleon. Our simulation results have demonstrated that both central collisions of the two extreme orientations can achieve full stopping and also form a bulk of hot, dense nuclear matter with a sufficiently large volume and long duration, because of the largely deformed uranium nuclei. The nucleon sideward flow in the tip-tip collisions is nearly three times larger than that in body-body ones at the normalized impact parameter $b/b_{\max} < 0.5$, and that the body-body central collisions have a large negative nucleon elliptic flow $v_2 = -12\%$ in contrast to zero in tip-tip ones. Thus the extreme circumstance and the novel experimental observables in tip-tip and body-body collisions can provide a good condition and sensitive probe for studying the nuclear EoS, respectively. The cooling storage ring (CSR) external target facility (ETF) to be built at Lanzhou, China, delivering a uranium beam up to 520 MeV/nucleon is expected to make a significant contribution to exploring the nuclear equation of state (EoS).

DOI: 10.1103/PhysRevC.76.044902 PACS number(s): 24.10.Lx, 25.75.Ld, 25.75.Nq, 24.85.+p

I. INTRODUCTION

In recent years, the ultrarelativistic high energy heavy ion collisions performed at the CERN Super Proton Synchrotron (SPS) and the BNL Relativistic Heavy Ion Collider (RHIC) ($\sqrt{s_{NN}} \sim$ 10–200 GeV) have focused on the high temperature and low baryon density region in the nuclear matter phase diagram [1] to search for a new form of matter with partonic degrees of freedom—the quark-gluon plasma (QGP) [2–5]. However, no dramatic changes of experimental observables, such as jet quenching, elliptic flow, and strangeness enhancement, have been observed yet [6]. On the other hand, the heavy ion collisions performed at the LBNL Bevalac facility and the GSI Schwerionen Synchrotron (SIS) [7,8] in the last two decades were used to produce hot and compressed nuclear matter to learn more about the nuclear equation of state (EoS) [9,10] at the high baryon density and low temperature region of the phase diagram. Although we have made great efforts to study the nuclear EoS, theoretically and experimentally, a solid conclusion can hardly be made. Therefore, it is still worthwhile to systematically study the collision dynamics as well as the EoS observables. Recently, to gain more understanding of the nuclear matter phase diagram and EoS at the high net-baryon density region, it has been proposed that uranium be collided on a uranium target at the external target facility (ETF) of the cooling storage ring (CSR) at Lanzhou, China, with a beam kinetic energy of 520 MeV/nucleon [11].

Uranium is the largest deformed stable nucleus and has an approximately ellipsoid shape with the long and short semiaxes given by $R_l = R_0(1 + 2\delta/3)$ and $R_s = R_0(1 - \delta/3)$, respectively, where $R_0 = 7$ fm is the effective spherical radius and $\delta = 0.27$ is the deformation parameter [12]. Consequently, one has $R_l/R_s = 1.3$. In our simulation, we consider two extreme orientations: the so-called tip-tip and body-body patterns with the long and short axes of two nuclei aligned to the beam direction, respectively [13], see Fig. 1 for illustration. The two types of orientations can be identified in random orientations of U+U collisions by making proper cutoffs in experimental data, such as the particle multiplicities, elliptic flow, and so on [11,14]. With the two extreme collision orientations, some novel stopping effects which are believed responsible for some significant experimental observables, such as particle production, collective motion, as well as attainable central densities, can be obtained. Because of the large deformation of the uranium nuclei [13,14], it is expected that the tip-tip collisions can form a higher density nuclear matter with longer duration than that formed in body-body or the spherical nuclei collisions, which is considered to be a powerful tool for studying the nuclear matter phase transition at high baryon density [13]; furthermore, the body-body central collisions may reveal a large out-of-plane elliptic flow (negative v_2) at high densities, which can be a sensitive probe for extracting the early EoS of hot, dense nuclear matter [13,15]. The novel experimental observables can be effectively utilized to study the possible nuclear matter phase transition and the nuclear EoS [9,10,13,15–20]. For comparing tip-tip and body-body collisions, a type of gedanken "sphere-sphere" collision without deformation of uranium nuclei is also included in the simulation.

The relativistic transport model ART1.0 [21,22] derived from the Boltzmann-Uehling-Uhlenbeck (BUU) model [23] has a better treatment of mean field and Pauli blocking effects [23] than cascade models [24]. The fragment production mechanism and partonic degrees of freedom are not present in the ART1.0 model. A soft EoS with the compressibility coefficient $K = 200$ MeV is used throughout the simulation, and the beam kinetic energy of uranium nuclei is set to 520 MeV/nucleon if not specifically indicated. In the next section, we discuss the stopping power ratio and selection of

*Contact author: science@mail.ustc.edu.cn

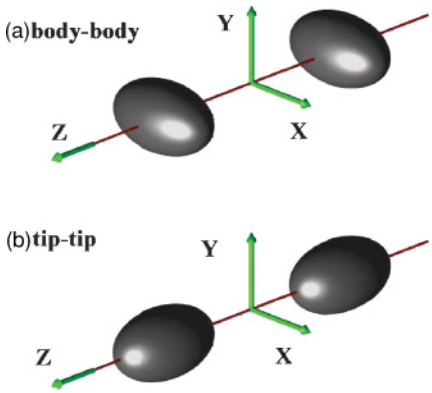

FIG. 1. (Color online) Two extreme collision orientations: (a) body-body and (b) tip-tip.

impact parameter **b**. In Sec. III, the evolution of baryon and energy densities and thermalization of central collision systems are studied. In Sec. IV, some experimental observables, such as nucleon sideward flow and elliptic flow, are also investigated. We summarize our results in Sec. V.

II. STOPPING POWER OF TIP-TIP AND BODY-BODY COLLISIONS

Large stopping power can lead to a remarkable pressure gradient in the compressed dense matter. It is generally also considered to be responsible for transverse collective motion [25], the maximum attainable baryon and energy densities, as well as the thermalization of collision systems. Thus, the study of the stopping power in U+U collisions may provide important information for understanding the nuclear EoS and collision dynamics.

A. Selection of impact parameter

The nuclear stopping power and geometric effects in U+U collisions rely strongly on the impact parameter **b**. Considering the conceptual design of the CSR-ETF detector [11], two methods are invoked here to estimate the impact parameter. The first one is the multiplicity of forward neutrons with polar angle $\theta < 20^\circ$ in the laboratory frame which can be covered by a forward neutron wall. The other method is to use the parameter $E_{\rm rat}$ [26], which is the ratio of the total transverse kinetic energy to the total longitudinal one, that is,

$$E_{\rm rat} = \sum_i E_{t_i} \Big/ \sum_i E_{z_i}. \tag{1}$$

The particles are also required to be within $\theta < 20^\circ$ in the laboratory frame, while the two qualities are calculated within the center-of-mass system (c.m.s.). The normalized impact parameter $b/b_{\rm max}$ is used to represent centralities of tip-tip and body-body collisions, and the $b_{\rm max}$ of the two cases are quite different from each other. As shown in Fig. 2, with either method, obvious linear dependence of the normalized impact parameter is demonstrated in both tip-tip and body-body near central collisions. Then, the two methods can be combined to determine the impact parameter to identify the most central collision events in both tip-tip and body-body collisions.

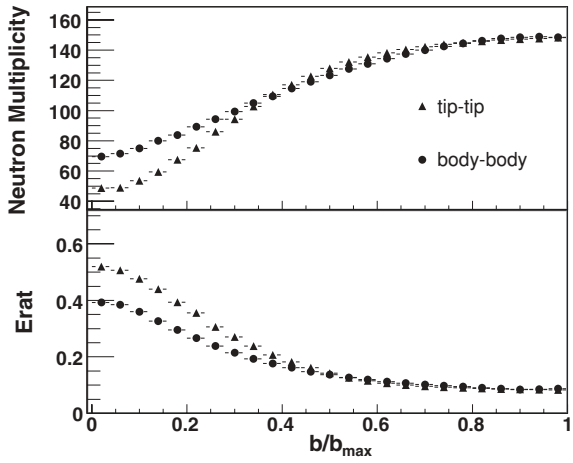

FIG. 2. Forward neutron multiplicity and $E_{\rm rat}$ as functions of normalized impact parameter $b/b_{\rm max}$ in both tip-tip and body-body collisions.

B. Stopping power ratio definition and evolution

It is difficult to obtain a universally accepted estimate of the nuclear stopping power in heavy ion collisions because of the proliferation of definitions of the concept [27]. The stopping power ratio R [28] is employed to measure the degree of stopping and is defined as

$$R = \frac{2}{\pi} \sum_j |P_{t_j}| \Big/ \sum_j |P_{z_j}|, \tag{2}$$

the total nucleon transverse momentum $|P_{t_j}|$ divided by the total absolute value of nucleon longitudinal momentum $|P_{z_j}|$ in the c.m.s. The ratio is widely used to describe the degree of thermalization and nuclear stopping by low and intermediate energy heavy ion collisions. It is a multiparticle observable on an event-by-event basis, which for an isotropic distribution is unity.

Figure 3 shows the time and normalized impact parameter dependence of the stopping ratio R for three conditions: tip-tip, body-body, and sphere-sphere collisions. When the ratio R reaches the value of 1, full stopping of the collision system is considered to be achieved, and the momenta are also in isotropy, which is not sufficient but necessary for thermal equilibrium of collision systems [28]. For $R > 1$, it can be explained by the preponderance of momentum flow perpendicular to the beam direction [29]. It is shown that all three conditions can achieve full stopping when the stopping ratio $R = 1$, the corresponding times for body-body and tip-tip central collisions are about 15 and 25 fm/c, respectively. Larger stopping ratios and faster evolution to full stopping are observed for body-body central collisions than for tip-tip and sphere-sphere ones at the early stage, which may indicate a more violent colliding process for body-body central collisions because of the sizable initial transverse overlap region. Although the stopping ratio of tip-tip central collisions

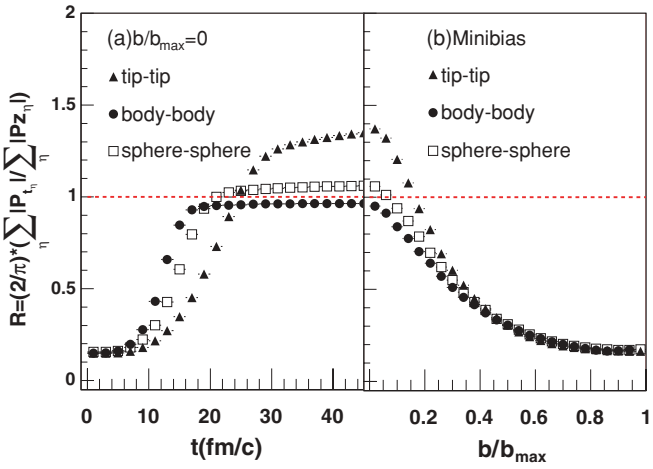

FIG. 3. (Color online) Stopping ratio R in tip-tip, body-body, and sphere-sphere central collisions as a function of (a) time and (b) $b/b_{\max}$ in minimum biased collisions.

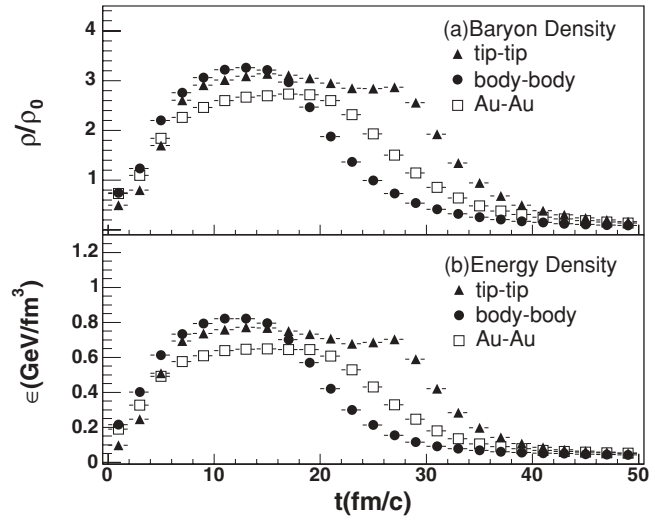

FIG. 4. Evolution of (a) baryon and (b) energy densities in tip-tip, body-body, and Au+Au central collisions.

is lower than the other two cases at the early time, it raises sharply later and even exceeds unity. So, it means that longer reaction and passage times can be obtained in tip-tip central collisions than in body-body and sphere-sphere ones, which may indicate the nucleons in tip-tip collisions can undergo more binary collisions to reach a higher transverse momentum.

In Fig. 3(b), the R of the three conditions gradually decrease with the increase in the normalized impact parameter. When $b/b_{\max} < 0.5$, the ratio is always larger for tip-tip collisions than for the other two cases, while for $b/b_{\max} > 0.5$ all three conditions have nearly the same stopping power ratio.

III. BARYON AND ENERGY DENSITIES AND THERMAL EQUILIBRIUM

Considering the discrepancy of stopping power between tip-tip and body-body collisions, it is interesting to study further the evolution of baryon and energy densities in both cases. As the full stopping and deformation effects occur in U+U collisions, it is believed that higher local baryon and energy density systems with long duration can be created, which is considered to be a significant condition for studying the nuclear EoS at the high baryon density region.

A. The evolution of baryon and energy densities

The evolution of baryon and energy densities in the central zone of tip-tip and body-body as well as Au+Au central collisions are illustrated in Fig. 4.

In Fig. 4, it is observed the maximum attainable baryon and energy densities for both tip-tip and body-body central collisions are about $3.2\rho_0$ and $0.8\ \mathrm{GeV/fm^3}$, respectively, while for the Au+Au collision they are about $2.6\rho_0$ and $0.6\ \mathrm{GeV/fm^3}$. Both the baryon and energy densities in U+U collisions are higher than the Au+Au one. Once a baryon density threshold of $\rho > 2.5\rho_0$ is required, the corresponding duration in tip-tip central collisions $\sim$20 fm/c (from $\sim$8 to $\sim$28 fm/c) is longer than the $\sim$10 fm/c (from $\sim$8 to $\sim$18 fm/c) of the body-body one, which is as predicted. But the peak densities have no significant discrepancy between the two cases, unlike those at the energy region of the Alternating Gradient Synchrotron (AGS) [13], which may be attributed to the full stopping at the CSR energy.

B. Thermalization of U+U collision systems

As mentioned before, the stopping ratio $R = 1$ is a necessary but not sufficient condition for thermal equilibrium of the collision system. To approach thermal equilibrium, a long duration of reaction is needed for nucleons to undergo sufficient binary collisions. As shown in Fig. 4(a), obvious long duration has been obtained in both tip-tip and body-body central collisions. It is therefore possible that thermal equilibrium at the time of freeze-out can be achieved.

Figure 5(a) is the evolution of the volume with a high baryon density ($\rho > 2.5\rho_0$) for tip-tip, body-body, and Au+Au central collisions, respectively. Both tip-tip and body-body central collisions have larger volumes than Au+Au one at the same beam kinetic energy of 520 MeV/nucleon. Although the maximum volume attainable for body-body central collisions ($\sim$220 fm^3) is about two times larger than the tip-tip one ($\sim$120 fm^3), the peak volume of tip-tip central collisions lasts a much longer time, $\sim$10 fm/c (from $\sim$15 to $\sim$25 fm/c), and is much more stable than the body-body one. To estimate the temperature at the freeze-out time, the scaled mean kinetic energy of all hadrons in a sphere of radius 2 fm around the system mass center is calculated as $\frac{2}{3}\langle E_k \rangle$ [22], which is utilized to reflect the thermalization temperature T of the collision system approximately. As illustrated in Fig. 5(b), both tip-tip and body-body central collisions show a flat region about 75 MeV, and the corresponding time ranges are about 10–28 and 10–18 fm/c, respectively. Considering the time range of the flat region in Fig. 5(b) associating with the corresponding range in Fig. 5(a) and also looking back at Fig. 4, we obtain a large volume of hot, dense nuclear matter in both tip-tip and body-body central collisions. Consequently, the extreme

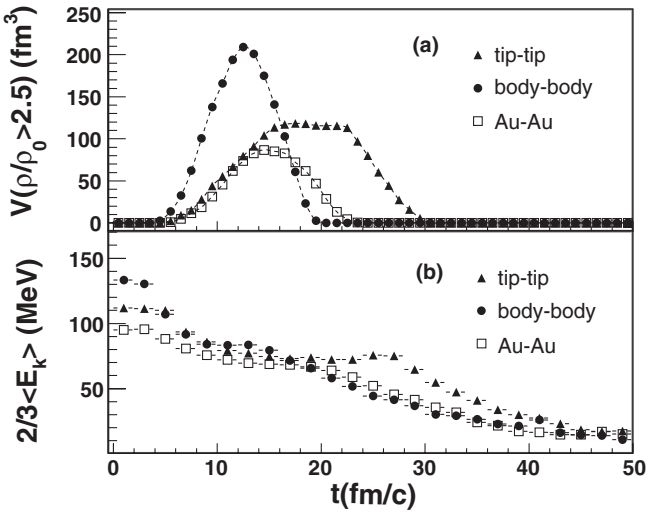

FIG. 5. Evolution of (a) volume with high density ($\rho > 2.5\rho_0$) in tip-tip, body-body, and Au+Au central collisions and (b) the scaled mean kinetic energy $\frac{2}{3}\langle E_k\rangle$, within a sphere of radius 2 fm around the system mass center.

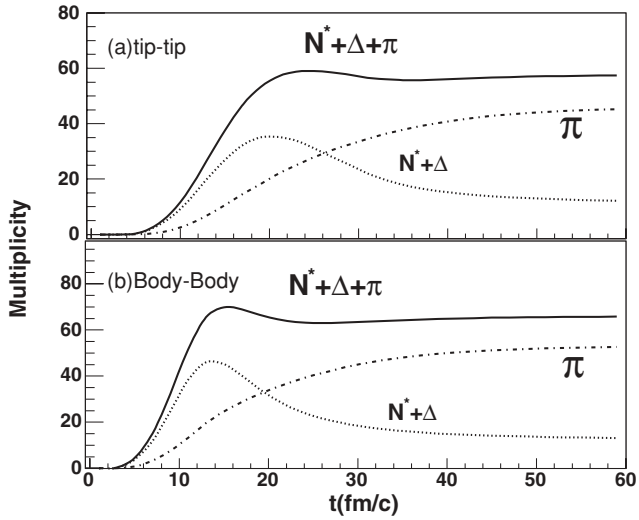

FIG. 6. Evolution of multiplicity of the free pion, $N^* + \Delta$, and $N^* + \Delta + \pi$ in (a) tip-tip and (b) body-body central collisions.

circumstance of sufficiently high temperature and density for a significantly large volume and long duration [13,22] has been formed in tip-tip and body-body central collisions, which condition can provide a good opportunity for studying the nuclear EoS as well as particles in medium properties, especially for the tip-tip case.

The time of freeze-out should be cautiously determined for estimating the thermalization temperature of a collision system. In Fig. 6, the multiplicity evolution of free pions which are not bounded in baryon resonances and pions still bounded inside the excited baryon resonances (Δ, N^*) (unborn pions) are displayed. At the Lanzhou CSR energy region (520 MeV/nucleon), the production and destruction of the Δ resonances are mainly through $NN \rightleftharpoons N\Delta$ and $\Delta \rightarrow N\pi$ reactions, in which the Δ decay rate is always higher than that of the formation of this resonance and the production of pion is predominated by the decay of the Δ resonances ($\Delta \rightarrow N\pi$) [30]. The total multiplicity of pion, Δ, and N^* approaches a saturated level after a period of evolution, indicating a freeze-out time of about $t = 28$ and $t = 18$ fm/c for tip-tip and body-body central collisions, respectively. The larger maximum attainable total multiplicity of pion, Δ, and N^* and freeze-out observed earlier indicates the existence of a faster evolution and more violent reaction process for the body-body central collisions than for the tip-tip case, which is consistent with the discussion before.

The corresponding temperature about 75 MeV at freeze-out time can be extracted from Fig. 5(b), for both tip-tip and body-body central collisions. To further confirm this estimation, the energy spectra of both the nucleon and the negatively charged pion are studied within the polar angle range of $90^\circ \pm 10^\circ$ in the c.m.s. The thermodynamic model [31] predicts that the energy spectra will be represented by a temperature T which characterizes a Maxwell-Boltzmann gas

$$\frac{d^2\sigma}{PE\,dE\,d\Omega} = \text{const} \times e^{-E_{\text{kin}}/T}, \tag{3}$$

where P and E are the particle momentum and total energy in the c.m.s.. Both the energy spectra and the Boltzmann fit results are shown in Fig. 7. The inverse slope (e.g., temperature T) of the nucleons in tip-tip and body-body central collisions are about 73 and 70 MeV, respectively, which are in good agreement with the temperatures extracted from Fig. 5(b) at the freeze-out time. The spectra of negatively charged pions show a different lower temperature than those of nucleons which may be explained by considering an equilibrated N and Δ system at thermal freeze-out and taking into account the kinematics of Δ decay [32]. The nucleon temperature closely

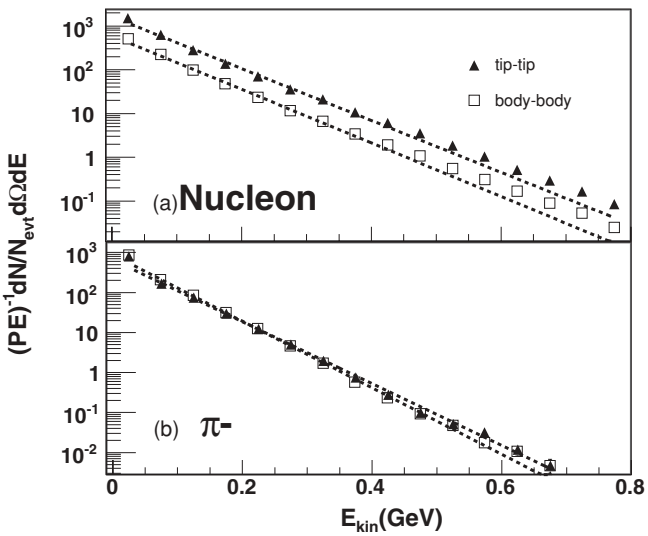

FIG. 7. Energy spectra of (a) nucleons and (b) negatively charged pions at $90^\circ \pm 10^\circ$ in the c.m.s. together with a Maxwell-Boltzmann fit for both tip-tip and body-body central collisions. The nucleon fit temperatures for tip-tip and body-body are about 73 and 70 MeV, respectively; those of the pion fit are about 56 and 52 MeV, respectively.

reflects the freeze-out temperature of tip-tip and body-body central collisions.

In conclusion, thermalization (or near thermalization) of the collision system corresponding to a freeze-out temperature of about 75 MeV is likely to be achieved in both tip-tip and body-body central collisions. However, it is also possible that the collision system is still in a nonequilibrium transport process on its path toward kinetic equilibration [30].

IV. THE COLLECTIVE FLOW OF U+U COLLISIONS

The stopping of nuclei in heavy ion collisions can lead to pressure gradients along different directions, resulting in a collective motion caused by spectator bounce-off [33] and participant squeeze-out effects [34]. Over the last two decades, at Bevalac and SIS energies, the so-called collective flow analysis has been established [16,33–36] to study the collective motion of the products in heavy ion collisions. The collective flow resulting from bounce-off and squeeze-out effects, which can be explained well by the hydrodynamics model [33,37] in good agreement with the experimental data, has been observed [38,39]. Because of the large deformation of the uranium nuclei, a novel collective motion is expected [13] and will be used to extract the medium properties and nuclear matter EoS information [15–20].

To perform flow analysis, it is necessary to construct an imaginary reaction plane defined by the direction of the beam (z) and the impact parameter vector $\mathbf{b}$ [40–42]. In our simulation, the x-z plane is just defined as the reaction plane with the beam direction along the z positive direction and the impact parameter vector $\mathbf{b}$ along the x positive direction. In last two decades, two methods have mainly been used to study the collective flow at the low and intermediate energies. One is the sphericity method [28,33,43,44] which yields the flow angle relative to the beam axis of the major axis of the best-fit kinetic energy ellipsoid, and the other employs the mean transverse momentum per nucleon projected into the reaction plane, $\langle p_x/A\rangle$, to perform a nucleon sideward flow analysis [40,45] which reflects the spectator bounce-off effects in the reaction plane. In recent years, an anisotropic transverse flow analysis method has usually been used. With a Fourier expansion [46,47] of the particle azimuthal angle ϕ distribution with respect to the reaction plane, different harmonic coefficients can be extracted, among which the first harmonic coefficient v_1, called directed flow (similar to sideward flow), and the second harmonic coefficient v_2, called elliptic flow, are the most interesting. The elliptic flow reflects the anisotropy of emission particles in the plane perpendicular to the reaction plane, while the directed flow describes the anisotropy in the reaction plane. The Fourier expansion can be expressed as

$$\frac{dN}{d\phi} \sim 1 + \sum_n 2v_n \cos(n\phi). \tag{4}$$

Figure 8 shows the nucleon sideward flow $\langle p_x/A\rangle$ for both tip-tip and body-body minimum biased collisions as a function of normalized rapidity, $y^{(0)} = Y_{\text{c.m.}}/y_{\text{c.m.}}$, in which $Y_{\text{c.m.}}$ represents the particle rapidity in c.m.s. and $y_{\text{c.m.}}$ is the rapidity of the system mass center. To extract the nuclear

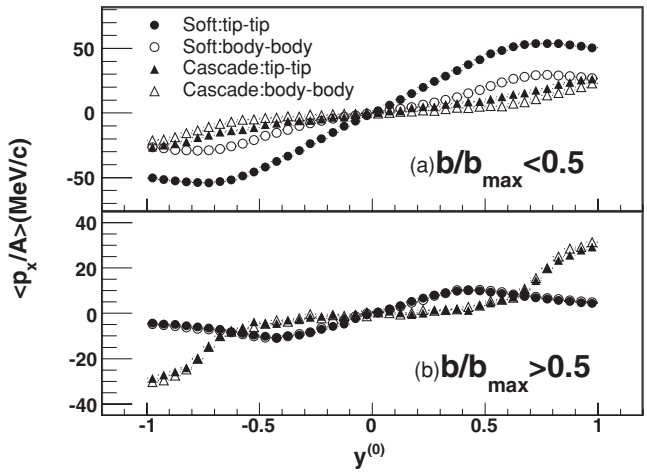

FIG. 8. Mean transverse momentum per nucleon projected into the reaction plane, $\langle p_x/A\rangle$, as a function of c.m.s. normalized rapidity for tip-tip and body-body collisions, with normalized impact parameter cutoffs (a) $b/b_{\max} \leqslant 0.5$ and (b) $b/b_{\max} > 0.5$.

EoS information and also demonstrate the discrepancies of the nucleon sideward flow in tip-tip and body-body collisions, cascade events [48], which neglect the mean field and Pauli blocking effects, are employed here to compare with the soft EoS case. In Fig. 8, with a soft EoS, it is noted that either tip-tip or body-body collisions show a spectator bounce-off effect revealing an obvious S shape [16,48] at the midrapidity region of $-0.5 < y^0 < 0.5$; while with the cascade one, an almost vanishing nucleon sideward flow appears. It can be understood that the nucleon sideward flow is related to the mean field, which is mainly responsible for the pressure gradient of the stopping nuclei, while the mean field has a strong dependence on the nuclear EoS. Therefore, the nucleon sideward flow is thought to be a good indirect probe for extracting the nuclear EoS information, especially in tip-tip case for its remarkable sideward flow. A cutoff on the normalized impact parameter is also applied to explore the impact parameter dependence of the nucleon sideward flow. As shown in Fig. 8(b), when $b/b_{\max} > 0.5$, the curves of the soft EoS and cascade are almost superposed with each other; while for $b/b_{\max} < 0.5$, a large discrepancy is observed in Fig. 8(a). The situation is quite similar to that in Fig. 3(b), which has almost the same stopping power for $b/b_{\max} > 0.5$ and a large discrepancy for $b/b_{\max} < 0.5$ in tip-tip and body-body minimum biased collisions, which means there exists a correlation between nuclear stopping power and sideward flow [49].

The normalized impact parameter dependence of the collective flow of nucleons is further studied by analyzing the flow parameter F [48] and the elliptic flow v_2 for both tip-tip and body-body as well as Au+Au minimum biased collisions. The flow parameter F is a quality customarily used to describe the nucleon sideward flow and is quantitatively defined as

$$F = \left.\frac{d\langle p_x/A\rangle}{dy^{(0)}}\right|_{y^{(0)}=0}, \tag{5}$$

the slope of the mean transverse momentum per nucleon projected into the reaction plane at $y^{(0)} = 0$.

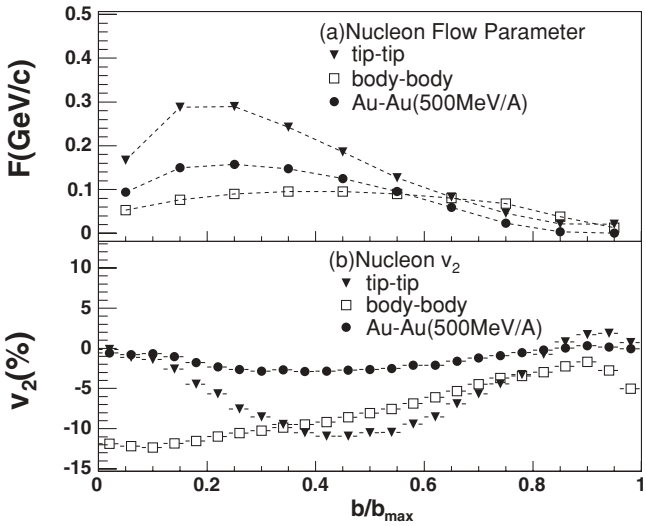

FIG. 9. (a) Nucleon flow parameter F and (b) c.m.s. midrapidity ($-0.5 < y^0 < 0.5$) nucleon elliptic flow v_2 of the three collision conditions as functions of the normalized impact parameter $b/b_{\max}$ with the soft EoS.

In Fig. 9(a), with $b/b_{\max} > 0.5$, the nucleon flow parameters F for tip-tip and body-body collisions have a similar value. This similarity, along with nearly the same stopping ratio R in Fig. 3(b), indicates the existence of similar pressure gradient effects on nucleon sideward flow in the two collision orientations. Whereas for $b/b_{\max} < 0.5$, the flow parameter F of tip-tip collisions is nearly three times larger than that of the body-body case. Even the sideward flow of Au+Au collisions is larger than the body-body one. It is further is confirmed that the tip-tip nucleon sideward flow is a more sensitive probe for extracting the information of nuclear EoS than that of the body-body one. The prominent high of the nucleon sideward flow in tip-tip collisions may result from the stronger pressure gradient between the participants and spectators in the reaction plane than in the body-body one, due to the largely deformed nuclei.

The normalized impact parameter dependence of nucleon elliptic flow v_2 at the midrapidity region ($-0.5 < y^0 < 0.5$) is displayed in Fig. 9(b). A significant negative v_2 at this energy region is consistent with the excitation function of the elliptic flow studied before [50]. The greatest negative v_2 of about -12% is observed in the body-body central collisions, which reflects the large geometric and squeeze-out effects in those collisions. While for tip-tip and Au+Au ones, the maximum negative v_2 are obtained at midcentrality. Both high baryon and high energy densities and large elliptic flow effects, which reflect an early EoS of the hot dense compression nuclear matter [15], are available in body-body central collisions. Thus, the body-body nucleon elliptic flow can also be taken as a sensitive probe of nuclear EoS. The novel behaviors of nucleon collective flows in tip-tip and body-body collisions are mainly attributed to the large deformation of the uranium nuclei.

V. SUMMARY

In summary, the CSR-ETF at Lanzhou provides a good opportunity to systematically study the nuclear EoS at the high net-baryon density region of the nuclear matter phase diagram. Due to the novel stopping effects in largely deformed U+U collisions, the simulation based on ART1.0 demonstrates that full stopping can be achieved and that a bulk of hot, high density nuclear matter with large volume and long duration can be formed in both tip-tip and body-body collisions. Large nucleon sideward flow in tip-tip collisions and the significant negative nucleon elliptic flow in body-body central collisions can provide a sensitive probe for extracting nuclear EoS information. Thus the extreme circumstances and the novel collective flow in both tip-tip and body-body collisions can provide good condition and sensitive probe for studying the nuclear EoS. More experimental observables of U+U collision dynamics should be further studied because of the geometric effects.

ACKNOWLEDGMENTS

We thank Bao-an Li, Feng Liu, Qun Wang, Zhi-Gang Xiao, and Nu Xu for their valuable comments and suggestions. This work is supported by National Natural Science Foundation of China (10575101,10675111). Supported by the CAS/SAFEA International Partnership Programme for Creative Research Teams under the grant number of CXTD-J2005-1.

[1] M. A. Stephanov, Int. J. Mod. Phys. A **20**, 4387 (2005).
[2] C. Lourenco *et al.*, Nucl. Phys. **A698**, 13 (2002).
[3] N. Xu *et al.*, Nucl. Phys. **A751**, 109 (2005).
[4] J. Adams *et al.*, Nucl. Phys. **A757**, 102 (2005).
[5] K. Adcox *et al.*, Nucl. Phys. **A757**, 184 (2005).
[6] P. Jacobs and X. N. Wang, Prog. Part. Nucl. Phys. **54**, 433 (2005).
[7] E. K. Hyde, Phys. Scr. **10**, 30 (1974).
[8] C. Höhne, Nucl. Phys. **A749**, 141c (2005).
[9] P. Danielewicz, arXiv:nucl-th/0512009.
[10] P. Danielewicz *et al.*, Science **298**, 1592 (2002).
[11] Z. G. Xiao, presented at 19th International Conference on Ultra-Relativistic Nucleus-Nucleus Collisions: Quark Matter 2006 (QM2006), Shanghai, China, 14–20 November 2006 (unpublished).
[12] A. Bohr and B. Mottelson, Nucl. Struct. **2**, 133 (1975).
[13] Bao-An Li, Phys. Rev. C **61**, 021903(R) (2000).
[14] E. V. Shuryak, Phys. Rev. C **61**, 034905 (2000).
[15] P. Danielewicz, R. A. Lacey, P. B. Gossiaux, C. Pinkenburg, P. Chung, J. M. Alexander, and R. L. McGrath, Phys. Rev. Lett. **81**, 2438 (1998).
[16] K. G. R. Doss *et al.*, Phys. Rev. Lett. **57**, 302 (1986).
[17] J. J. Molitoris *et al.*, Nucl. Phys. **A447**, 13c (1985).
[18] J. Hofmann *et al.*, Phys. Rev. Lett. **36**, 88 (1976).
[19] H. Stöocker and W. Greiner, Phys. Rep. **137**, 277 (1986).
[20] H. Stöocker *et al.*, Z. Phys. A **290**, 297 (1979).
[21] Bao-An Li and C. M. Ko, Phys. Rev. C **52**, 2037 (1995).
[22] Bao-An Li *et al.*, Int. J. Mod. Phys. E **10**, 267 (2001).
[23] G. F. Bertsch and S. D. Gupta, Phys. Rep. **160**, 189 (1988).

[24] J. Cugnon, Phys. Rev. C **22**, 1885 (1980).
[25] A. Andronic *et al*., Eur. Phys. J. A **30**, 1 (2006).
[26] B. Hong *et al*., Phys. Rev. C **66**, 034901 (2002).
[27] S. P. Sorensen *et al*., presented at Conference: 21. International Symposium on Multiparticle Dynamics, Wuhan, China, 23–27 September 1991, Rep. No. CONF-9109221-3:DE92009006 (1991).
[28] H. Ströbele *et al*., Phys. Rev. C **27**, 1349 (1983).
[29] R. E. Renfordt, D. Schall, *et al*., Phys. Rev. Lett. **53**, 763 (1984).
[30] Bao-An Li and W. Bauer, Phys. Rev. C **44**, 450 (1991).
[31] J. Gosset, H. H. Gutbrod, W. G. Meyer, A. M. Poskanzer, A. Sandoval, R. Stock, and G. D. Westfall, Phys. Rev. C **16**, 629 (1977).
[32] R. Brockmann *et al*., Phys. Rev. Lett. **53**, 2012 (1984).
[33] H. A. Gustafsson *et al*., Phys. Rev. Lett. **52**, 1590 (1984).
[34] H. H. Gutbrod, K. H. Kampert, B. Kolb, A. M. Poskanzer, H. G. Ritter, R. Schicker, and H. R. Schmidt, Phys. Rev. C **42**, 640 (1990).
[35] R. E. Renfordt *et al*., Phys. Rev. Lett. **53**, 763 (1984).
[36] H. Stöcker, J. A. Maruhn, and W. Greiner, Phys. Rev. Lett. **44**, 725 (1980).
[37] H. Stöcker *et al*., Phys. Rev. Lett. **47**, 1807 (1981).
[38] W. Scheid *et al*., Phys. Rev. Lett. **32**, 741 (1974).
[39] G. Buchwald, G. Graebner, J. Theis, J. Maruhn, W. Greiner, and H. Stocker, Phys. Rev. Lett. **52**, 1594 (1984).
[40] P. Danielewicz and G. Odyniec, Phys. Lett. **B157**, 146 (1985).
[41] J. Y. Ollitrault, Phys. Rev. D **48**, 1132 (1993).
[42] R. J. M. Snellings *et al*., STAR Note 388, 1999 (unpublished).
[43] J. Cugnon *et al*., Phys. Lett. **B109**, 167 (1982).
[44] M. Gyulassy *et al*., Phys. Lett. **B110**, 185 (1982).
[45] H. A. Gustafsson *et al*., Z. Phys. A **321**, 389 (1985).
[46] A. M. Poskanzer and S. A. Voloshin, Phys. Rev. C **58**, 1671 (1998).
[47] S. A. Voloshin and Y. Zhang, Z. Phys. C **70**, 665 (1994).
[48] F. Rami *et al*., Nucl. Phys. **A646**, 367 (1999).
[49] W. Reisdorf *et al*., Phys. Rev. Lett. **92**, 232301 (2004).
[50] J. Y. Ollitrault, Nucl. Phys. **A638**, 195 (1998).